Biochimica et Biophysica Acta, 771 (1984) 1–8
Elsevier

BBA 72011

EFFECT OF EXTERNAL AMMONIUM ON THE KINETICS OF THE SODIUM CURRENT IN FROG MUSCLE

D. ŠUPUT *

I. Physiologisches Institut der Universität des Saarlandes, D-6650 Homburg/Saar (F.R.G.)

(Received October 6th, 1983)

Key words: Voltage clamp; Intracellular pH; Na^+ current; NH_4^+ effect; (Frog muscle)

(1) The effect of externally applied 20 mM NH_4Cl on steady-state Na^+ inactivation h_∞ and other electrical parameters has been studied in voltage-clamped frog muscle fibres. (2) Exposure to Ringer with 20 mM NH_4Cl causes a small transient shift of the $h_\infty(E)$ curve to more positive potentials. Upon return to normal Ringer the $h_\infty(E)$ curve shifts in the opposite direction, overshooting its original position, and then returns slowly into the original position. (3) Similar but smaller shifts of the descending branch of the $I_{Na}(E)$ curve, of the $P_{Na}(E)$ curve and of the time to peak curve are also observed. (4) The shifts are thought to result from the changes in intracellular pH which occur during and after NH_4Cl application. The observations are compatible with the idea that intracellular pH affects the surface charge potential at the inner side of the membrane.

Introduction

Ammonium ions have for a long time attracted the interest of neurologists and electrophysiologists. Elevated blood ammonium concentrations are thought to cause malfunction of the central nervous system [1]. Ammonium ions depolarize nerve and muscle fibres [2,3] and are able to move through sodium and potassium channels [4–8]. They reversibly depress post-synaptic inhibition [9]. In cardiac Purkinje fibres, addition of 5 mM NH_4Cl to the Tyrode solution produces a 10 mV shift of the activation curve of the i_{K_2} current [10].

As shown by measurements with intracellular pH electrodes [11–15], exposing nerve cells or muscle fibres to a solution with NH_4Cl causes a rapid rise of intracellular pH, pH_i, due to NH_3 entry. It is followed by a slower fall of pH_i produced by the entry of NH_4^+. On return to normal Ringer pH_i rapidly decreases and overshoots its original value because ammonium ions move outward as NH_3 and leave H^+ in the cytoplasm. In a mouse soleus muscle fibre, 20 mM NH_4^+ causes a transient increase of the intracellular pH from 6.9 to 7.1 and a rebound acidification to 6.5 [13].

The shift of the activation curve of the i_{K_2} current in Purkinje fibres by 5 mM NH_4Cl is thought to be due to intracellular alkalinization and increase in negative surface charge on the inside of the membrane [10]. The present paper describes shifts of the steady-state sodium inactivation curve in voltage-clamped frog skeletal muscle fibres during and after exposure to Ringer solution with 20 mM NH_4Cl. The shifts are transient and biphasic; their direction is compatible with the idea that external NH_4Cl affects the surface charge on the inside of the membrane through changes of the intracellular pH.

* Send reprint request to D. Šuput at (present address): Patofiziološki inštitut; Medicinska fakulteta, Zaloška 4, 61105 Ljubljana, Slovenija, Yugoslavia.

Abbreviations: EGTA, ethylene glycol bis(β-aminoethyl ether)-*N*,*N*'-tetraacetic acid; Mes, 4-morpholineethanesulfonic acid; Mops, 4-morpholinepropanesulfonic acid.

Methods

Experiments were done on short pieces of single muscle fibres dissected from the m. semitendinosus of the frog *Rana esculenta*. Muscles were stretched and mounted in a dissection dish containing standard Ringer solution (see Table I). The Ringer was then replaced by a depolarizing solution of following composition: 60 mM K_2EGTA, 10 mM NaF and 30 mM CsF, pH 7.4. This solution facilitates dissection as, following a short period of 'fibrillation', it prevents further twitching of the muscle. Otherwise the dissection and mounting of fragments of single muscle fibres was similar to the procedure described before [16]. The four pools of a perspex cell were filled with one of the artificial intracellular solutions listed in Table I. The investigated portion of the membrane ('artificial node') was located in the A-pool of the perspex cell. After mounting of the fibre the solution in this pool was replaced by one of the extracellular bathing solutions listed in Table I. All external solutions contained tetraethylammonium ions and all internal solutions contained Cs ions to eliminate K^+ currents.

'Artificial nodes' were voltage clamped at 14°C, using a method decribed before [17–18] which allows compensation for the resistance in series with the membrane (R_s). The membrane potential was held at approximately −90 mV at which h_∞ was 0.9 at the beginning of an experiment. Membrane currents were recorded across a constant resistor of 470 $k\Omega$ and through a 25 kHz low pass filter on film or sampled at intervals of 10 μs by a DEC PDP 11/23 computer equipped with A/D and D/A converters and programmable clocks of the company Data Translations.

Leakage and capacitative current were compensated electronically by an analogue circuit at the beginning of each experiment. Usually the amplitude of the leakage current changed during the course of an experiment. It increased markedly but reversibly during the application of NH_4Cl. These changes of leakage current were corrected off-line with the computer. For this purpose the current produced by a hyperpolarizing pulse was suitably scaled and subtracted from the Na^+ current records. When there was a pronounced nonlinearity in the leakage current-voltage relation, the current associated with a small depolarizing pulse was used instead.

R_s was compensated as far as possible. Usually the elimination of the instantaneous voltage step in the current clamp [16] was taken as criterion for the correct setting of R_s compensation. Further compensation led to a serious distortion of the shape of sodium currents [16] and was therefore avoided.

As shown in Fig. 1A, the series resistance R_s shifts the descending branch of the $I_{Na}(E)$ curve to the left along the voltage axis. The artifact produced by R_s is largest for large currents. Therefore, in most experiments the membrane currents were diminished by decreasing the Na_o/Na_i ratio,

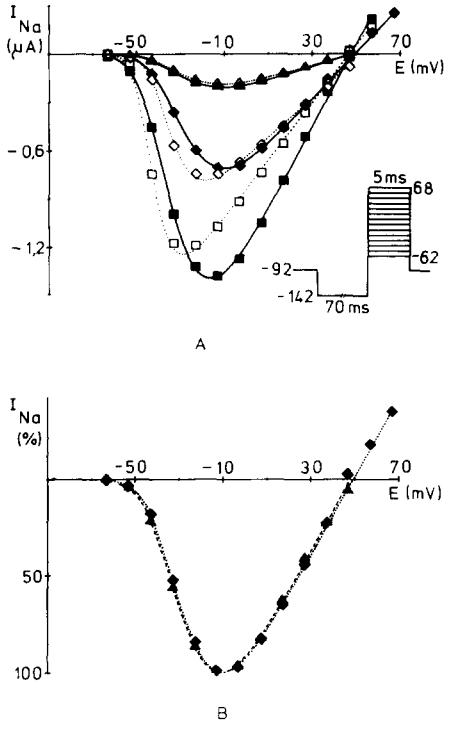

Fig. 1. Effect of series resistance R_s on the $I_{Na}(E)$ curve. (A) Open symbols represent currents measured without R_s compensation, filled symbols currents measured with optimally compensated R_s. Pool A perfused with K^+-free Ringer (□, ■) or with K-free Ringer plus 3.5 nM tetrodotoxin (△, ▲). Points ◇ and ◆ obtained after partial wash-out of tetrodotoxin. All other pools filled with 90 mM CsF. Pulse sequence shown in inset. (B) Curves ▲ and ◆ from A are scaled to the same amplitude of I_{Na} to show perfect elimination of R_s artifact when Na^+ current amplitude does not exceed 700 nA and R_s is optimally compensated.

TABLE I

COMPOSITION OF ARTIFICIAL INTRACELLULAR SOLUTIONS (A) AND BATHING SOLUTIONS (B)

A: Artificial intracellular solutions

Solution	CsF (mM)	NaF (mM)	K_2EGTA (mM)	Tris-HCl (mM)	Mops (mM)	Mes (mM)	pH
85 mM CsF	85	10	10	4	–	–	7.4
90 mM CsF	90	5	10	4	–	–	7.4
100 mM Mops	40	5	10	–	100	–	7.35
100 mM Mes	40	5	10	–	–	100	5.7

B: Bathing solutions

Solution	NaCl (mM)	$CaCl_2$ (mM)	KCl (mM)	TEA [a] (mM)	Tris-HCl (mM)	Choline chloride (mM)	NH_4Cl [b] (mM)	pH
Ringer	100	1.8	2.5	–	5	–	–	7.4
K^+-free Ringer	100	1.8	–	11	5	–	–	7.4
Na^+-poor Ringer	40	2.0	–	10	4	65	–	7.35
Na^+-poor Ringer with NH_4Cl	45	2.0	–	10	4	40	20	7.35

[a] Tetraethylammonium.

[b] NH_4Cl was added each time to the solution from a stock solution of 1 M NH_4Cl. This did not alter the pH by more than 0.05 pH units.

using artificial intracellular solutions containing 5 or 10 mM NaF and bathing solutions with no more than 45 mM NaCl. When the largest currents were in the range of 700 nA or less, R_s could be completely compensated (Fig. 1B). All the currents analyzed were well below 700 nA, i.e. the results are practically not contaminated by R_s artifacts.

The composition of the external and internal solutions is given in Table I. In most experiments the external bathing solution was either Na^+-poor Ringer or Na^+-poor Ringer with NH_4Cl; the latter solution contained slightly more Na^+ than the former in order to compensate for a weak depressing action of NH_4Cl on the Na^+ currents (see Results, this page). The internal solution in these experiments was 85 or 90 mM CsF buffered to pH 7.4 with 4 mM Tris-HCl; the buffering power of the internal solution (1.4 mequiv. H^+/pH unit per liter at pH 6.2–7.1) was small compared to the buffering power of the cytoplasm of a mouse muscle fibre (45 mequiv. H^+/pH unit per liter) [19]. In additional experiments the effect of an acid internal solution (100 mM Mes, pH 5.7) was studied; a strongly buffered neutral solution (100 mM Mops, pH 7.35) served as control.

The junction potential at the agar bridge in pool A changed by less than 0.1 mV when Na^+-poor Ringer was replaced by Na^+-poor Ringer with NH_4Cl.

Results

1. Shift of the steady-state inactivation curve

Changing from Na^+-poor Ringer with 40 mM NaCl to Na^+-poor Ringer with 40 mM NaCl and 20 mM NH_4Cl had two immediate effects: a reversible increase of leakage current, also seen by previous authors [8,9], and a slight decrease of the Na^+ inward current. The correction for the increase in leakage current has been described under Methods. To avoid the decrease of the Na^+ inward current and the corresponding change of $I_{Na} \cdot R_s$ the Na^+ concentration of the Na^+-poor Ringer with NH_4Cl was routinely increased to 45 mM (see Table I).

In the first series of experiments the effect of external NH_4Cl on the steady-state inactivation curve, $h_\infty(E)$, was studied. To measure the $h_\infty(E)$

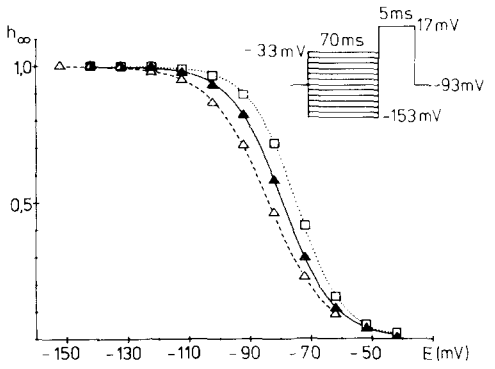

Fig. 2. Shift of steady-state inactivation curve after addition and wash-out of NH_4Cl. Pulse programme see inset. Normalised test pulse current I_{Na} is plotted against membrane potential during 70 ms conditioning pulse. ▲, Na^+-poor Ringer; □, Na^+-poor Ringer with NH_4Cl for 90 s; △, 120 s after return to Na^+-poor Ringer. Cut ends of fibre in 90 mM CsF (+5 mM NaF). Points fitted with Eqn. 1. E_h is −78.3, −74.2 and −83.0 mV for ▲, □ and △, respectively.

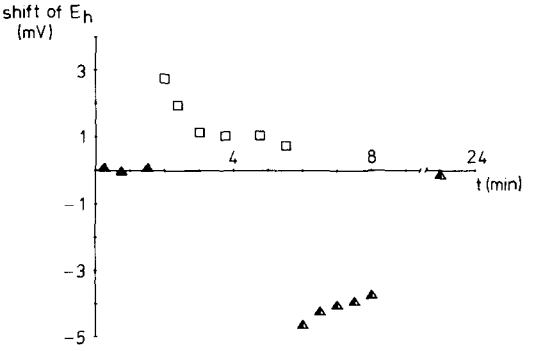

Fig. 3. Shift of E_h as a function of time. ▲, Na^+-poor Ringer; □, Na^+-poor Ringer with NH_4Cl; △, return to Na^+-poor Ringer. In the first minute after application of NH_4Cl E_h shifts by 3 mV and then moves back towards the control value. Wash-out of NH_4Cl results in a rapid shift of −5.4 mV. Afterwards E_h returns slowly to its normal value.

curve 70 ms conditioning pulses to varying potentials followed by a constant test pulse were used (see pulse programme in Fig. 2). In order to minimize the effect of series resistance on the $h_\infty(E)$ curve, a test pulse potential (17 mV) in the ascending branch of the $I_{Na}(E)$ curve was chosen [20]. Normalised test pulse current was plotted against membrane potential during conditioning pulse. The equation

$$h_\infty = \frac{1}{1 + \exp\left(\frac{E - E_h}{k}\right)} \qquad (1)$$

was fitted to the experimental points. In this equation k is the slope parameter and E_h is the potential at which $h_\infty = 0.5$.

Fig. 2 shows three $h_\infty(E)$ curves. The middle curve (▲) is the control curve in Na^+-poor Ringer without NH_4Cl; its E_h is −78.3 mV, similar to the value of −79 mV reported earlier [21]. Curve □ was measured 90 s after application of Na^+-poor Ringer with 20 mM NH_4Cl and is shifted to the right ($E_h = -74.2$ mV). Upon returning to Na^+-poor Ringer without NH_4Cl the $h_\infty(E)$ curve moves to the left (symbols △, $E_h = -83.0$ mV), overshooting its original position. Compared with curve □ the curve △ is shifted 8.8 mV to the left.

The shift of the $h_\infty(E)$ curve is strongly time dependent. Fig. 3 shows repeated measurements of E_h before (▲), during (□) and after (▲) application of NH_4Cl. On the ordinate the shift of E_h relative to the control values ▲ is plotted. The largest shift of E_h occurs in the first minute of application or wash-out. Afterwards E_h drifts back towards the control value. 'Recovery' of E_h is faster during application of NH_4Cl than during wash-out. The total amplitude of the change in E_h is 7.5 mV.

The average (± standard error of the mean) of E_h was -75.5 ± 1.1 mV under control conditions ($n = 14$). The average shift of E_h (observed in the first minute after solution change) was 3.7 ± 0.65 mV in NH_4Cl and -4.2 ± 0.62 mV during wash-out. The total amplitude of the shift was on the average 7.9 ± 0.35 mV.

The slope parameter k was 8.32 ± 0.22 mV. The slope of the $h_\infty(E)$ curve did not significantly change in NH_4Cl ($k = 8.18 \pm 0.22$ mV) but decreased slightly during wash-out ($k = 9.15 \pm 0.22$ mV); the latter effect was completely reversible.

2. Shift of the $I_{Na}(E)$ curve

The descending branch of the $I_{Na}(E)$ curve shifted in the same direction as the $h_\infty(E)$ curve, but the shift was usually smaller. Fig. 4 shows $I_{Na}(E)$ curves from the same experiment as in Fig. 2. Symbols ▲, □ and △ refer to measurements before application of NH_4Cl, after 8 min in Na^+-

poor Ringer with NH_4Cl and 3 min after return to Na^+-poor Ringer, respectively. NH_4Cl shifts the descending branch of the $I_{Na}(E)$ curve by 2.6 mV without altering its slope. During wash-out the curve is shifted -5 mV from its original position, i.e. -7.6 mV relative to its position during NH_4Cl application. The maximum Na^+ inward current remained practically constant. The reversal potential was 48 mV in control; i.e. close to its theoretical value of 57 log (40/5) = 51 mV; it increased by 2.4 mV during application of Na^+-poor Ringer with NH_4Cl and returned to its original value during wash-out.

From the Na^+current I_{Na} the Na^+ permeabilities P_{Na} were calculated by means of the constant-field equation and plotted against membrane potential E (Fig. 5), using the same symbols as in Fig. 4. The curves rise steeply for small depolarizations and level off above 0 mV, in agreement with earlier measurements [21]. The shifts (measured at $P_{Na} = 1 \cdot 10^{-8}$ cm^3/s) during and after NH_4 application are 3 and -6.5 mV, respectively, similar to the values 2.6 and -7.6 mV obtained from the descending branches of the $I_{Na}(E)$ curves.

Similar observations were made on a total of ten fibres. The average shift during NH_4^+ application was 3.2 ± 0.5 mV. In seven out of the ten fibres the $I_{Na}(E)$ curve shifted to the left of its original position during wash-out. The increase of reversal potential during application of Na^+-poor Ringer with NH_4Cl amounted to 2–3 mV and is mainly attributed to the slightly higher Na^+ concentration of this solution.

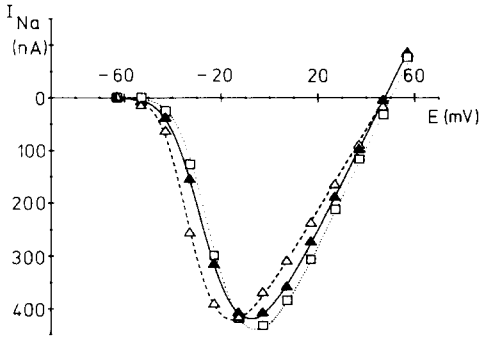

Fig. 4. $I_{Na}(E)$ curve in Na^+-poor Ringer (▲), after 8 min in Na^+-poor Ringer with NH_4Cl (□) and 3 min after return to Na^+-poor Ringer (△). Holding potential -93 mV. All depolarizations were preceded by a 70 ms pulse to -143 mV. Same fibre as in Fig. 2.

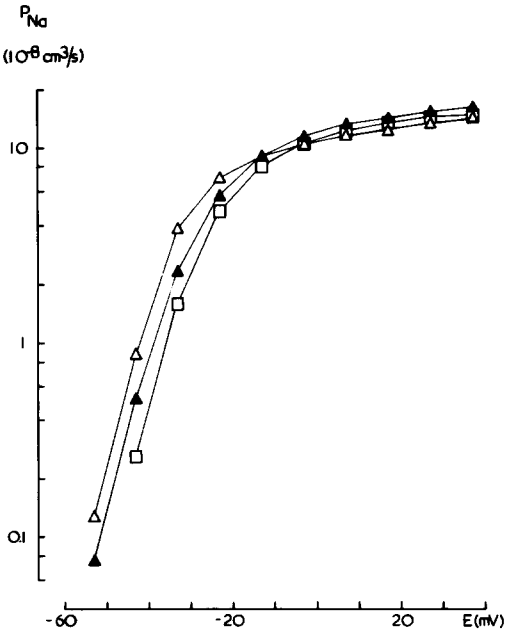

Fig. 5. $P_{Na}(E)$ curve in Na^+-poor Ringer (▲), after 8 min in Na^+-poor Ringer with NH_4Cl (□) and 3 min after return to Na^+-poor Ringer (△). Same experiment as in Fig. 4. The permeabilities P_{Na} were calculated from the currents I_{Na} by means of the constant field equation, using a value of 48 mV (▲, △) or 50.5 mV (□) for the apparent equilibrium potential E_{Na}.

3. Effect on the time course of Na^+ currents

Fig. 6A shows superimposed Na^+ inward currents during a depolarizing pulse from -90 to -30 mV in Na^+-poor Ringer with NH_4Cl (faint curve) and after return to Na^+-poor Ringer (heavy curve). The time to peak was 0.76 ms in Na^+-poor Ringer with NH_4Cl and 0.58 ms in Na^+-poor Ringer. Fig. 6B gives the relation between time to peak and pulse potential before (▲), during (□) and after (△) application of NH_4Cl. Over the whole potential range the time to peak is longer during application of NH_4Cl than before; during wash-out it becomes slightly shorter than under control conditions. The increase of time to peak in Na^+-poor Ringer with NH_4Cl accompanied the positive shift of the descending branch of the $I_{Na}(E)$ curve.

There was no significant change in the decay

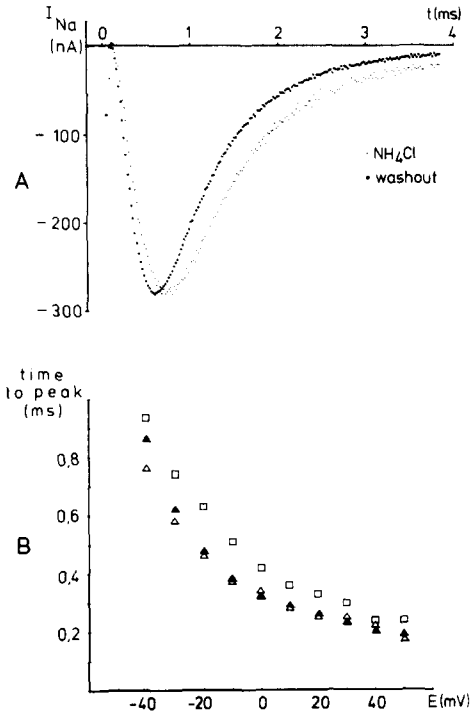

Fig. 6. Effect of NH_4Cl on the time-course of the Na^+ inward current. (A) Na^+ inward current associated with a pulse from -90 to -30 mV after 90 s in Na^+-poor Ringer with NH_4Cl (faint curve) and 3 min after return to Na^+-poor Ringer (heavy curve). (B) Time to peak as a function of pulse potential in Na^+-poor Ringer (▲), in Na^+-poor Ringer with NH_4Cl (□) and 3 min after return to Na^+-poor Ringer (△).

rate of the Na^+ inward current during application of Na^+-poor Ringer with NH_4Cl (see Fig. 6A). A marked slowing of Na^+ inactivation could, however, be achieved by applying a strongly buffered acid solution to the cut ends of the fibre, a procedure also used in previous work [22]. The effect of the acid solution developed gradually over 30–60 min. Fig. 7 shows the Na^+ inward current associated with a 4 ms pulse to -30 mV before (A) and 75 min after (B) application of 100 mM Mes, pH 5.7 to the cut ends. In B, the time to peak is increased and the decay of I_{Na} is markedly slowed; at the end of the 4 ms pulse I_{Na} has only decayed to 30% of its peak value. The change in kinetics was accompanied by a decrease of the Na^+ current amplitude; the original amplitude could, however, be restored by a hyperpolarizing prepulse (see Fig. 7B). The effect of the acid solution was almost completely reversible upon re-application of a neutral solution to the cut ends (Fig. 7C). It became, however, irreversible and more pronounced when the acid solution was applied for more than about 75 min; the exact time varied considerably due to variations in fibre diameter and length. The effect of the acid solution (100 mM Mes, pH 5.7) was the same whether 90 mM CsF, pH 7.4 (as in Fig. 7) or 100 mM Mops, pH 7.35 was used as neutral control solution.

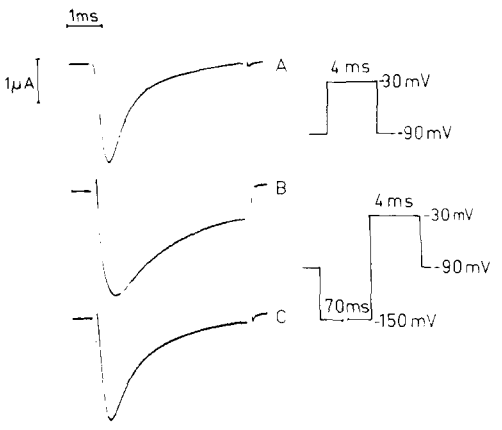

Fig. 7. Change of I_{Na} after application of acid solution to the cut ends of the fibre for 75 min. Solution on cut ends: A, 90 mM CsF, pH 7.4; B, 100 mM Mes, pH 5.7 for 75 min; C, 20 min after return to 90 mM CsF, pH 7.4. External solution: K^+-free Ringer. Pulse programme as shown; in B and C a hyperpolarizing prepulse was used to obtain a full-size I_{Na}.

4. Measurement of internal pH

Intracellular pH, pH_i, of cut muscle fibres was measured by recessed-tip pH-sensitive microelectrodes. Both a pH-sensitive and a conventional microelectrode were inserted into the same fibre as described previously [19]. The fibre was superfused with Na^+-poor Ringer and the cut ends of the fibre were in 90 mM CsF. Under these conditions pH_i was 6.74 (range 6.65–6.80, $n = 5$). Following application of Na^+-poor Ringer with 20 mM NH_4Cl pH_i rapidly rose to 7.10–7.40 ($n = 5$). Upon returning to Na^+-poor Ringer without NH_4Cl pH_i fell to 6.25–6.40 ($n = 4$) and then slowly rose again.

These results which are similar to those reported previously [13] were obtained on unclamped muscle fibres. Unfortunately, the vaseline seals used in the voltage clamp apparatus blocked the recess of the pH-sensitive microelectrodes, so it

proved impossible to perform pH_i measurements on fibres clamped at −93 mV.

Discussion

The experiments show that exposure to 20 mM NH_4Cl causes a small transient shift of the $h_\infty(E)$ curve to more positive potentials (average 3.7 mV), followed during wash-out by a larger shift in the opposite direction (average −7.9 mV) and a slow subsequent return to the original position. These shifts of the $h_\infty(E)$ curve are accompanied by similar but smaller shifts of the descending branch of the $I_{Na}(E)$ curve, of the $P_{Na}(E)$ curve and of the curve relating time to peak to membrane potential.

The observed shifts of the electrical parameters are similar in time course to the changes in pH_i which occur in a frog or mouse muscle fibre during application of 20 mM NH_4^+ and during rebound acidification (see Results p. 6 and Fig. 2 in Ref. 13). It therefore seems likely that the shifts of the electrical parameters are a result of the changes in pH_i.

From the pH_i measurements the amplitude of the pH_i change responsible for the voltage shift of −7.9 mV is estimated as 0.6–1.0 pH units. This estimate is subject to uncertainty since the actually occurring pH_i change in a voltage-clamped muscle fibre is not exactly known. Likewise, the shift of the electrical parameters may have been underestimated because the size of the shift is strongly dependent on time.

The direction of the observed voltage shifts is consistent with the idea that an increase of pH_i increases and a decrease of pH_i decreases the internal surface charge potential. Experiments on internally perfused squid giant axons have demonstrated that variations of internal pH from 4.8 to 11 result in voltage shifts of the kinetic parameters of the Na and K system which can be satisfactorily explained in terms of the Gouy-Chapman-Stern equation applied to the diffuse double layer generated by fixed surface charges at the inner side of the membrane [23].

The voltage shifts observed during and after exposure to 20 mM NH_4Cl are similar in magnitude to the shifts produced by small changes in external pH. As shown in Table IV and Fig. 5 of Ref. 21, changing the external pH from 7.4 to 6.0 or 9.4 shifts the $P_{Na}(E)$ curve of the muscle fibre membrane by 4.8 and −3.2 mV, respectively.

The experiments described here support the idea that external NH_4Cl can affect the excitability parameters through a change of the surface charge on the inside of the membrane. The shifts observed in frog skeletal muscle fibres are smaller than those reported for cardiac Purkinje fibres [10], perhaps due to a higher intracellular buffering power. To obtain a marked slowing of inactivation it was necessary to apply a strongly buffered acid solution to the cut ends of the fibre for one hour or more (see Fig. 7 and Ref. 22). It is, however, possible that the effects developing during long lasting strong lowering of pH_i are not primarily caused by H^+ but are due to secondary processes, e.g. release of lysosomal proteases.

Acknowledgement

This work was supported by the Deutsche Forschungsgemeinschaft (SFB 38) and by the Research Community of Slovenija. I am grateful to Professor H. Meves for continuous encouragement and for reading the manuscript and to Dr. R.C. Thomas in whose laboratory I was able to make the pH_i measurements. I am also indebted to Dr. D. Hof and O. Schneider for help with the computer and to Dr. W. Schwarz for advice.

References

1 Goodman, L.S. and Gilman, A. (1980) The Pharmacological Basis of Therapeutics, 6th Edn., Macmillan, New York
2 Höber, R. and Strohe, H. (1929) Pflügers Arch. 222, 70–88
3 Shanes, A.M. (1958) Pharmacol. Rev. 10, 59–164
4 Lüttgau, H.C. (1961) Pflügers Arch. 273, 302–310
5 Binstock, L. and Lecar, H. (1969) J. Gen. Physiol. 53, 342–361
6 Hille, B. (1971) J. Gen. Physiol. 58, 599–619
7 Hille, B. (1973) J. Gen. Physiol. 61, 669–686
8 Campbell, D.T. (1976) J. Gen. Physiol. 67, 295–307
9 Aickin, C.C., Deisz, R.A. and Lux, H.D. (1982) J. Physiol. 329, 319–339
10 Van Bogaert, P.P., Vereecke, J.S. and Carmeliet, E.E. (1978) Pflügers Arch. 375, 45–52
11 Thomas, R.C. (1974) J. Physiol. 238, 159–180
12 Boron, W.F. and DeWeer, P. (1976) J. Gen. Physiol. 67, 91–112
13 Aickin, C.C. and Thomas, R.C. (1977) J. Physiol. 273, 295–316

14 Deitmer, J.W. and Ellis, D. (1980) J. Physiol. 304, 471–488
15 Moody, W.J. (1981) J. Physiol. 316, 293–308
16 Hille, B. and Campbell, D.T. (1976) J. Gen. Physiol. 67, 265–293
17 Nonner, W. (1969) Pflügers Arch. 306, 176–192
18 Schwarz, W., Neumcke, B. and Palade, P.T. (1981) J. Membrane Biol. 63, 85–92
19 Aickin, C.C. and Thomas, R.C. (1977) J. Physiol. 267, 791–810
20 Goldman, L. and Schauf, C.L. (1972) J. Gen. Physiol. 59, 659–675
21 Campbell, D.T. and Hille, B. (1976) J. Gen. Physiol. 67, 309–323
22 Nonner, W., Spalding, B.C. and Hille, B. (1980) Nature 284, 360–363
23 Carbone, E., Testa, P.L. and Wanke, E. (1981) Biophys. J. 35, 393–413